Reprinted from the *Soil Science Society of America Proceedings*
Volume 37, no. 3, May-June 1973
677 South Segoe Rd., Madison, Wis. 53711 USA

Steady-State Seepage in a Hillside

G. C. A. MORIN AND A. W. WARRICK

Steady-State Seepage in a Hillside[1]

G. C. A. MORIN AND A. W. WARRICK[2]

ABSTRACT

The complex potential function is obtained for two-dimensional seepage of water through a hillside using conformal transformations. Two cases are considered: In the first a straight slope of finite length intersects an infinitely wide horizontal plane; in the second, a horizontal plane of finite width is between two symmetric hillsides. Flow nets and graphical relations characterize the flow patterns.

Additional Index Words: infiltration, conformal transformations, drainage, saturated flow.

THIS PAPER presents a mathematical solution describing the two-dimensional seepage of water from a hillside adjoining a flat horizontal plane at its lower end. The complex potential is found as a function of position and can be used to determine the hydraulic potential, the stream function, and the velocity distribution. This information is useful in gaining a better understanding of flow in sloping soil masses. Kirkham (1947) discussed field measurements showing flow into and from similar hillside surfaces in an Iowan drift area. The flow velocity and direction are closely related to movement of chemical constituents into and from the soil surface, amount of subsurface flow vs. surface flow, erosion hazards and seepage spots.

The geometry *ABCDA* as given in the *z*-plane of Fig. 1 is considered. A hillside is inclined at an angle of $\pi\alpha$ radians with respect to the adjoining horizontal surface of seepage *CD*. The hill extends to the right a distance *L* to a barrier or symmetry plane *AB*. We assume there is sufficient water supplied at the surface of the soil mass to maintain saturation within the entire flow region. The flow region has a uniform hydraulic conductivity, *k* (units of length per time), throughout.

A similar problem was solved by Warrick (1970) where the seepage surface *CD* was chosen to be a mirror image of *CB* and the *y*-axis a line of symmetry. Klute, Scott, and Whisler (1965) presented a solution for a saturated sloping rectangular slab and Whisler (1969) later used an electric analog in the study of associated unsaturated cases. Powers, Kirkham and Snowden (1967) and Selim and Kirkham (1972) solved similar problems by generating a series of orthogonal functions using the Gram-Schmidt process. The present method satisfies the specified boundary conditions exactly and gives an analytical solution (at least in terms of an exact integral). In the Gram-Schmidt procedures the boundary conditions are satisfied at discrete nodes rather than continuously, although very arbitrary boundary conditions are allowable.

We define the complex potential function $w(x,y)$ by

$$w(x,y) = k\phi(x,y) + i\psi(x,y) \qquad [1]$$

where $\phi(x,y)$ is the hydraulic head function (units of length), $\psi(x,y)$ the stream function (units of volume per unit time per unit length), and i the imaginary unit vector. Each of the functions ϕ, ψ, and w satisfies Laplace's equation. Also $k\phi$ and ψ are conjugate functions and are everywhere orthogonal in the *z*-plane. Following the method described by Davison and Rosenhead (1940) and by Polubarinova-Kochina (1962), we define a Zhukovsky function θ by

$$\theta = w/kL + iz/L \qquad [2]$$

where $z = x + iy$. The real and imaginary parts of θ may be found from [1] and are:

$$\theta_1 = (\phi - y)/L \qquad [3a]$$

$$\theta_2 = (\psi/k + x)/L. \qquad [3b]$$

The region in the θ-plane which corresponds to the flow region is the shaded area in Fig. 1. The barrier *AB* is defined by $\psi = 0$ and $x = L$ in the *z*-plane and corresponds to $\theta_2 = 1$ in the θ-plane. Along the surface of seepage *BCD*, we have $\phi = y$ which corresponds to the line $\theta_1 = 0$ in the θ-plane. Points *A* and *D* correspond to infinity in both the θ and *z*-planes.

Also shown in Fig. 1 is a *t*-plane which is useful to relate the *z* and θ-planes. When a correspondence of *z* to *t* and of

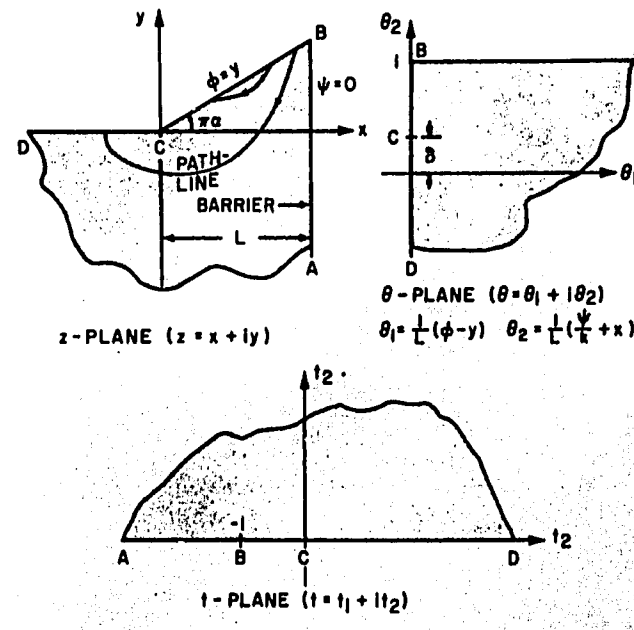

Fig. 1—The *z*, θ, and *t* planes for an infinitely wide horizontal plane adjacent to a finite slope.

[1] Arizona Agricultural Experiment Station Paper 1993. Support was from Arizona Projects 0206-4151-94 and the US Agency for International Development (211d grant). Received Oct. 24, 1972. Approved Jan. 5, 1973.

[2] Graduate Research Associate and Associate Professor, respectively, Dep. of Soils, Water & Engineering, Univ. of Arizona, Tucson 85721.

θ to t are established, the relationship of z to θ and of z to w is known by use of [2]. As the regions of interest in both the θ and the t-plane are polygons (each with one vertex at infinity), we may use Schwartz-Christoffel transformations (as in Churchill, 1960) to develop the mapping functions onto the t-plane. For convenience, we place points A and D at infinitiy in the t-plane and B and C at -1 and zero, respectively.

We may write the differential forms of the transformations as

$$d\theta = M_\theta' \, (t+1)^{-3/2} \, dt \qquad [4]$$

$$dz = M_z' \, (t+1)^{-1/2-\alpha} \, t^\alpha \, dt \qquad [5]$$

where M_θ' and M_z' are constants which give the proper scaling and orientation for the polygons.

Integrating each side of [4] gives

$$\theta(t) = M_\theta \, (t+1)^{1/2} + N_\theta \qquad [6]$$

with M_θ and N_θ as constants. At point B we have $\theta = i$ and $t = -1$, thus N_θ is given as

$$N_\theta = i. \qquad [7]$$

Point C maps onto the θ-plane at $\theta = i\delta$, where δ will be calculated below. Point C also corresponds to $t = 0$, therefore we find from [6] and [7] that

$$M_\theta = -i(1-\delta). \qquad [8]$$

Thus, [6] becomes

$$\theta(t) = i[1 - (1-\delta)\,(t+1)^{1/2}]. \qquad [9]$$

The inverse of [9] is found by solving for t:

$$t = -\left(\frac{\theta - i}{1-\delta}\right)^2 - 1. \qquad [10]$$

A comparison of [4] and [5] gives

$$dz = M_z[t/(t+1)]^\alpha \, d\theta. \qquad [11]$$

In order to evaluate the constant M_z, we first examine the derivative $d\theta/dz$. Use of [1] and [2] gives

$$\frac{d\theta}{dz} = -\frac{v_x}{kL} + i\frac{v_y}{kL} + \frac{i}{L} \qquad [12]$$

where v_x and v_y are the horizontal and vertical velocity components. As θ approaches infinity the velocity terms v_x and v_y approach zero. Thus, [11] and [12] for θ and t approaching infinity give

$$M_z = -iL. \qquad [13]$$

Use of [13] in [11] and integrating [11] from $z = 0$ and $\theta = i\delta$ results in

$$z = -iL \int_{i\delta}^{\theta} \left[1 + \left(\frac{1-\delta}{\theta - i}\right)^2\right]^\alpha d\theta. \qquad [14]$$

Let us consider the integral of [14] in two segments, one section from $\theta = i\delta$ to $\theta = i\theta_2$ and the other from $\theta = i\theta_2$ to $\theta = \theta_1 + i\theta_2$. Thus [14] is equivalent to:

$$z/L = (z/L)_{BCD} + I_S + iI_C \qquad [15]$$

where

$$(z/L)_{BCD} = \int_{\delta}^{\theta_2} \left[1 - \left(\frac{1-\delta}{\theta_2 - 1}\right)^2\right]^\alpha d\theta_2 \qquad [16]$$

and

$$I_S + iI_C = -i \int_0^{\theta_1} \left\{1 + \left[\frac{1-\delta}{\theta_1 + i(\theta_2 - 1)}\right]^2\right\}^\alpha d\theta_1. \qquad [17]$$

The first integral of [15] corresponds to z/L along the seepage surface BCD whereas the sum is the value of z/L for an interior point.

Defining η by

$$\eta = (1-\theta_2)^2/(1-\delta)^2 \qquad [18]$$

[16] becomes

$$(z/L)_{BCD} = [(1-\delta)/2] \int_\eta^1 (\eta - 1)^\alpha \, \eta^{-\alpha-1/2} \, d\eta. \qquad [19]$$

Along the sloping surface CB, $z = x \sec \pi\alpha \exp(i\pi\alpha)$ and $(\eta - 1)^\alpha = \exp(i\pi\alpha)\,(1-\eta)^\alpha$.

Thus, in terms of real numbers only

$$(x/L)_{CB} = [(1-\delta)/2] \int_\eta^1 (1-\eta)^\alpha \, \eta^{-\alpha-1/2} \, d\eta \qquad [20a]$$

$$(y/L)_{CB} = \tan \pi\alpha \, (x/L)_{CB} \qquad [20b]$$

or

$$(x/L)_{CB} = [(1-\delta)/2]\,[B(1+\alpha, 0.5-\alpha) - B_\eta\,(1+\alpha, 0.5-\alpha)] \qquad [21]$$

where the incomplete Beta function and ordinary Beta function are given as in Abramowitz and Stegun (1964, esp. p. 258 and 263):

$$B_\eta(a,b) = \int_0^\eta \rho^{a-1}\,(1-\rho)^{b-1} \, d\rho \qquad [22]$$

$$B(a,b) = B_1\,(a,b) = \Gamma(a)\,\Gamma(b)/\,\Gamma(a+b) \qquad [23]$$

where $\Gamma(a)$, $\Gamma(b)$, and $\Gamma(a+b)$ are Gamma functions.

The unknown parameter δ may be evaluated by observing that point B corresponds to $x = L$, $\theta_2 = 1$ and $\eta = 0$. Thus, from [16] and [18] we find

$$1 = [(1-\delta)/2]\,B(1+\alpha, 0.5-\alpha).$$

Solving for δ and using $\Gamma(1.5) = \pi^{1/2}/2$ and [23] gives

$$\delta = 1 - \frac{\pi^{1/2}}{\Gamma(1+\alpha)\,\Gamma(0.5-\alpha)}. \qquad [24]$$

Along the horizontal seepage surface CD, we can show from [22]

$$(x/L)_{CD} = -[2/(1-\delta)] \int_{1/\eta}^{1} (1-U)^{\alpha}\, U^{-3/2} dU \qquad [25]$$

where U is a dummy integration variable and η is given by [18]. In the limit as η approaches infinity (x approaches point D), the integral in [25] is undefined as it should be; for finite values of η, the corresponding x/L is finite.

The integrals I_S and I_C of [17] may be written as

$$I_S = \int_0^{\theta_1} R \sin\beta \, d\theta_1 \qquad [26]$$

and

$$I_C = -\int_0^{\theta_1} R \cos\beta \, d\theta \qquad [27]$$

with the magnitude R as

$$R = \left\{ 1 + \left(\frac{(1-\delta)^2 [\theta_1^2 - (\theta_2 - 1)^2]}{D} \right)^2 + \left(\frac{2(1-\delta)^2 \theta_1 (\theta_2 - 1)}{D} \right)^2 \right\}^{\alpha/2} \qquad [28]$$

with

$$D = [\theta_1^2 - (\theta_2 - 1)^2]^2 + 4\theta_1^2 (\theta_2 - 1)^2 \qquad [29]$$

and the angle β as

$$\beta = \alpha \tan^{-1} \left\{ \frac{2(1-\delta)^2 \theta_1 (\theta_2 - 1)}{D + (1-\delta)^2 [\theta_1^2 - (\theta_2 - 1)^2]} \right\}, \; 0 \le \beta \le \pi. \qquad [30]$$

The horizontal and vertical flow velocities can be evaluated using [12]:

$$v_x / kL = -\text{Real}\,(d\theta / dz) \qquad [31a]$$

$$v_y / kL = -(1/L) + \text{Imag}\,(d\theta / dz) \qquad [31b]$$

where

$$\frac{d\theta}{dz} = \frac{1}{L} \left[1 + \left(\frac{1-\delta}{\theta - i} \right)^2 \right]^{-\alpha}. \qquad [32]$$

Along the sloping surface CB where $\theta = i\theta_2$ and $\delta < \theta \le 1$, [31a], [31b] and [32] give

$$\left(\frac{v_x}{k}\right)_{CB} = -\cos \pi\alpha \left[\left(\frac{1-\delta}{1-\theta} \right)^2 - 1 \right]^{-\alpha} \qquad [33a]$$

$$\left(\frac{v_y}{k}\right)_{CB} = -1 + \sin \pi\alpha \left[\left(\frac{1-\delta}{1-\theta_2} \right)^2 - 1 \right]^{-\alpha} \qquad [33b]$$

Along the horizontal surface CD, $v_x = 0$ and v_y is

$$\left(\frac{v_y}{k}\right)_{CD} = -1 + \left[1 + \left(\frac{1-\delta}{1-\theta_2} \right)^2 \right]^{-\alpha}. \qquad [33c]$$

The flow velocity normal to the surface v_N may be determined from known v_x and v_y values by

$$v_N = -v_x \sin \pi\alpha + v_y \cos \pi\alpha. \qquad [33d]$$

Solutions for a Finite Width Between Two Hillsides

Consider as in Fig. 2, two adjacent hillsides CB and EF separated by a finite distance of $2a$ and with the y-axis chosen along the plane of symmetry. The solution of this problem is similar to the simpler problem already considered in this paper and less detail will be given to its derivation. For the special case of $a = 0$, this problem is that considered by Warrick (1970). As "a" approaches infinity the problem is the same as for Fig. 1 although [15] is not readily obtainable from the solution we seek now. If the value of ψ is chosen as zero along AB, then ψ will also be zero along the negative y-axis and FG. The hydraulic head ϕ will be equal to y along the surface $BCDEF$. The flow region of the z-plane will correspond to the semi-infinite strip in the θ-plane and the upper half of the t-plane as before. We will choose for A, B, C, and D the image points $t = -\infty$, -1, $-c$ and 0, respectively. Image points for E, F, and G will be c, 1, and ∞ by symmetry.

The differentials of the transformations for θ and z to the t-plane are

$$d\theta = M_\theta (t+1)^{-1/2} (t-1)^{-1/2} \, dt \qquad [34]$$

and

$$dz = M_z' (t+1)^{-1/2-\alpha} (t+c)^{\alpha} (t-c)^{\alpha} (t-1)^{-1/2-\alpha} \, dt. \qquad [35]$$

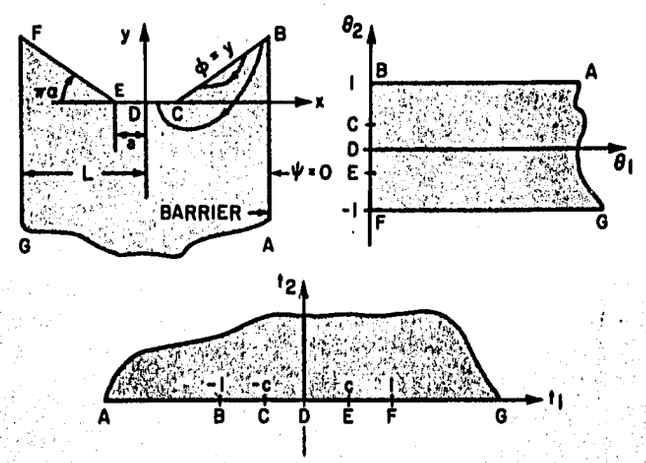

Fig. 2—The z, θ, and t planes for a finite spacing between two hillsides.

Integrating [34] and evaluating M_θ using $\theta = 0$ at $t = 0$ and $\theta = i$ at $t = -1$, we obtain

$$\theta(t) = -(i2/\pi)\sin^{-1}t. \qquad [36]$$

The inverse of [36] is

$$t = i\sinh(\pi\theta/2). \qquad [37]$$

Use of [34] and [37] in [35] leads to

$$dz = M_z\left[\frac{\sinh^2(\pi\theta/2) + c^2}{\sinh^2(\pi\theta/2) + 1}\right]^\alpha d\theta. \qquad [38]$$

The scaling constant M_z is determined in the same manner as for the infinitely wide horizontal plane, in fact, M_z is given by [13] as $M_z = -iL$. As $\theta = 0$ corresponds to $z = 0$, we have

$$z = -iL\int_0^\theta\left[\frac{\sinh^2(\pi\theta/2) + c^2}{\sinh^2(\pi\theta/2) + 1}\right]^\alpha d\theta \qquad [39]$$

or alternatively

$$z/L = -i\int_0^\theta[1 - (1 - c^2)\,\mathrm{sech}^2(\pi\theta/2)]^\alpha\, d\theta. \qquad [40]$$

Along the surface DC, we have $\theta = i\theta_2$ and $\sinh(\pi\theta/2) = i\sin\theta_2$. Thus, for $x = a$ (Point C) we have from [39]

$$\frac{a}{L} = \int_0^{\frac{2}{\pi}\sin^{-1}c}\left(\frac{c^2 - \sin^2(\pi\theta_2/2)}{1 - \sin^2(\pi\theta_2/2)}\right)^\alpha d\theta_2 \qquad [41a]$$

or

$$a/L = \int_0^c (c^2 - \rho^2)^\alpha (1 - \rho^2)^{\alpha - 1/2}\, d\rho \qquad [41b]$$

where ρ is a dummy integration variable. Either [41a] or [41b] may be used to determine the unknown c by trial and error. Values of c for a range of a/L and α values will be given in Table 2.

The results for interior points x/L and y/L are

$$\frac{x}{L} = \frac{a}{L} + \cos\pi\alpha\, I' + \int_0^{\theta_1} R'\sin\beta'\, d\theta_1 \qquad [42a]$$

$$\frac{y}{L} = \sin\pi\alpha\, I' - \int_0^{\theta_1} R'\cos\beta'\, d\theta \qquad [42b]$$

where

$$I' = \int_{(2/\pi)\sin^{-1}c}^{\theta_2}\left(\frac{\sin^2(\pi\theta_2/2) - c^2}{1 - \sin^2(\pi\theta_2/2)}\right)^\alpha d\theta_2 \qquad [42c]$$

$$\beta' = \alpha\tan^{-1}\left[\frac{-2(1 - c^2)\,\tau\sigma}{1 - (1 - c^2)(\tau^2 - \sigma^2)}\right] \qquad [42d]$$

$$R' = \{[1 - (1 - c^2)(\tau^2 - \sigma^2)]^2 + 4(1 - c^2)^2\tau^2\sigma^2\}^{\alpha/2} \qquad [42e]$$

with

$$\tau = \frac{\cosh(\pi\theta_1/2)\cos(\pi\theta_2/2)}{\cosh^2(\pi\theta_1/2)\cos^2(\pi\theta_2/2) + \sinh^2(\pi\theta_1/2)\sin^2(\pi\theta_2/2)} \qquad [42f]$$

$$\sigma = \frac{-\sinh(\pi\theta_1/2)\sin(\pi\theta_2/2)}{\cosh^2(\pi\theta_2/2)\cos(\pi\theta_2/2) + \sinh^2(\pi\theta_1/2)\sin^2(\pi\theta_2/2)}. \qquad [42g]$$

For the sloping surface CB, [42a] and [42b] simplify to

$$(x/L)_{CB} = a/L + \cos\pi\alpha\, I' \qquad [43a]$$

$$(y/L)_{CB} = \sin\pi\alpha\, I'. \qquad [43b]$$

Numerical Calculations and Results

In order to calculate ϕ and ψ relationships for interior points of the infinitely wide case (Fig. 1), the following steps are useful:

1) Specify α

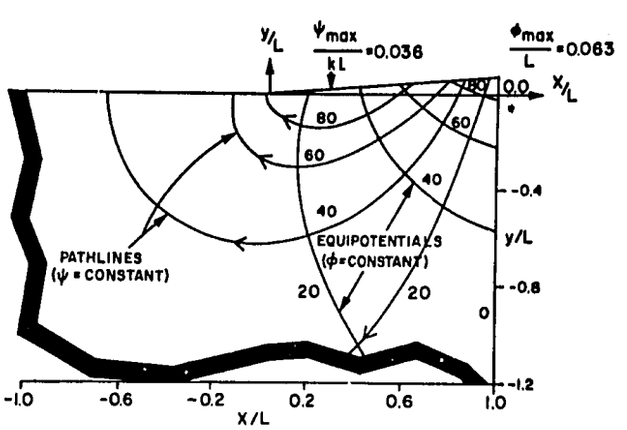

Fig. 3a—Flow net for the infinitely wide case, where $\alpha = 0.02$ (slope of 3.6 degrees).

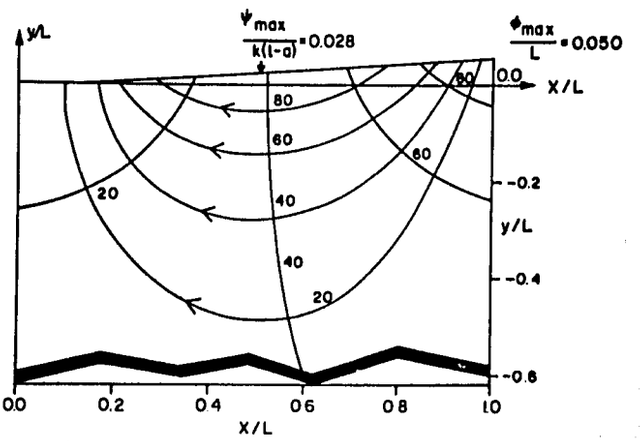

Fig. 3b—Flow net for the finitely wide case with $\alpha = 0.02$ and $a/L = 0.2$. The y/L axis is a symmetry line.

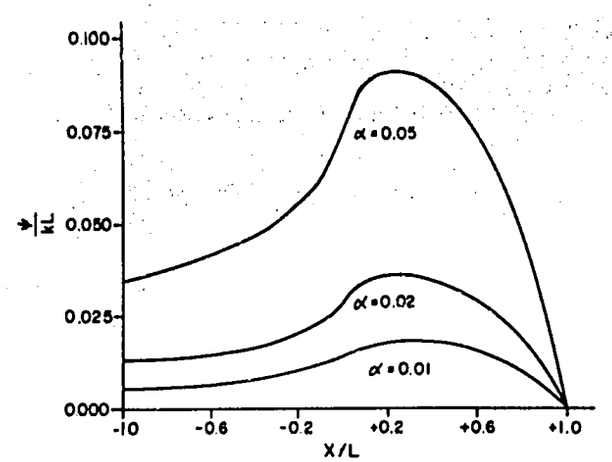

Fig. 4a—ψ/kL as a function of the surface position x/L for $\alpha = 0.01$, 0.02, and 0.05.

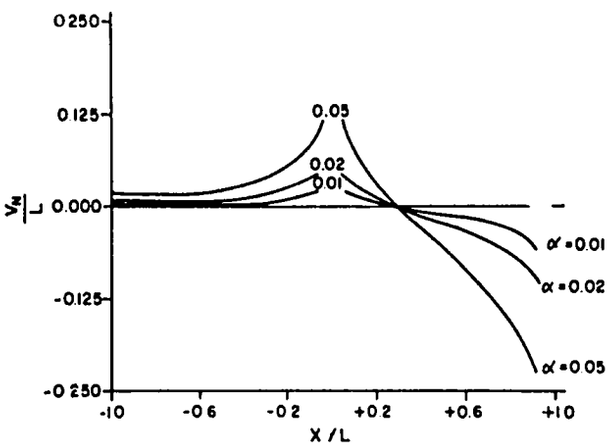

Fig. 4b—Normal flux (v_N/L) through the flow media surface for $\alpha = 0.01$, 0.02, and 0.05. The flux is taken as positive for flow out of the soil surface.

2) Calculate δ from [24]
3) Assign θ_1 and θ_2. Each θ_1 and θ_2 corresponds to a specific point; θ_1 can have any positive value, θ_2 can have values between $-\infty$ and 1.
4) Solve for $z/L = (x + iy)/L$ using [15]. (The actual computational formulas used for computation are [20a] and [20b] or [25], [26], and [27]).
5) Solve for ϕ/L and ψ/kL from [3a] and [3b]:

$$\phi/L = \theta_1 + y/L, \quad \psi/kL = \theta_2 - x/L.$$

The flow net of Fig. 3a was prepared for $\alpha = 0.02$ (3.6 degree slope) using the steps outlined above. The Gamma functions of [24] were evaluated using the polynomial approximation of Abramowitz and Stegun (1964), eq. 6.1.36). The integrals of [20a], [20b], [25], [26], and [27] were numerically evaluated using a "trapezoidal" procedure by McCracken and Dorn (1964, p. 189, exer. 20). The integrands of [20a], [20b], [26], and [27] are undefined at the upper right corner (Point B). However, the integrals are well behaved and were evaluated in the region close to Point B using the leading terms of series approximations to the integrals. Three terms gave negligible round-off error.

The equipotentials shown in Fig. 3a are for 20, 40, 60, and 80% of the maximum value of $\phi/L = 0.063$ which occurs at the upper right-hand corner of the flow medium. The minimum value of ϕ is zero and occurs all along the negative x-axis. The streamlines are also labeled 20, 40, 60, and 80%. The maximum value of $\psi/kL = 0.036$ occurs at $x/L = 0.29$ and is taken as 100%. This point, $x/L = 0.29$, is labeled in the figure and is the dividing point for seepage into the surface (all points upslope) and seepage out of the surface (all points below). All of the streamlines originate from the upper portion of the slope. Streamlines 40, 60, and 80 come back out on the flat horizontal surface to the left of the origin as would the 20% streamline if the x-axis were extended beyond $x/L = -1.0$. The right-hand portion of Fig. 3a is somewhat similar to that of Klute, Scott and Whisler (1965, Fig. 2) for the upper half of a tilted slab where a line perpendicular to the surface and passing through the middle of the slab is an equipotential.

Table 1—Values of $Q/2kL$ and x_{max}/L for infinitely wide case of Fig. 1

Angle α	Angle Degrees	$Q/2kL$	x_{max}/L
0.01	1.8	0.018	0.30
0.02	3.6	0.036	0.30
0.03	5.4	0.054	0.29
0.04	7.2	0.073	0.28
0.05	9.0	0.091	0.27
0.06	10.8	0.11	0.26
0.07	12.6	0.13	0.26
0.08	14.4	0.15	0.25
0.09	16.2	0.17	0.24
0.10	18.0	0.19	0.23
0.20	36.0	0.39	0.16
0.30	54.0	0.61	0.099
0.40	72.0	0.81	0.044
0.49	88.2	0.98	0.0039

Figures 4a and 4b are plots of ψ/kL and v_N/k along the soil surface and verify some of the above statements. The maximum value of ψ/kL (read from the $\alpha = 0.02$ curve) is 0.036 and occurs at $x/L = 0.29$. The normal flux reverses sign at $x/L = 0.29$. The flux is taken as negative for flow into the column, positive for flow out. The value of ψ/kL and v_N/k are also shown for $\alpha = 0.01$ (1.8 degrees) and 0.05 (9 degrees). No value of v_N/k is given at $x/L = 0$ because the velocity is undefined at this point. The magnitudes of v_N and ψ tend to be greater for steeper slopes. This does not say steep slopes take in more water for a given rainfall rate, but merely that more water will be taken in on a steep slope which is kept saturated than on a lesser slope. Table 1 gives the maximum values of ψ/kL, that is, the values $Q/2kL$ and x_{max}/L and the coordinate where ψ reaches its maximum values for a wider range of α.

The flow net shown in Fig. 3b was prepared using a procedure similar to that for Fig. 3a. This flow net is representative of those for a finite width between two hillsides. The value of a/L is 0.2 and α is chosen as 0.02, the same slope as was used for Fig. 3a. The major difference from Fig. 3a is that the streamlines are forced to return to the soil surface before they reach the symmetry plane (along the y-axis). The maximum value of ψ occurs at $x/L = 0.52$. When ψ is normalized with respect to the slope width ($L-a$ for Fig. 2) we find $\psi_{max}/k(L-a) = 0.028$ which may be compared directly to the 0.036 from Fig. 3a. This gives a numerical verification of the fact that more flow will occur in a slope without restriction to force water to the surface a finite distance from the base of the slope as in Fig. 3b.

Table 2—Values of c, $Q/2kL$, and ψ/kL for various α, a/L and slope positions for the finite width case of Fig. 2

Angle					ψ/kL for selected x/L values					
α	Degrees	a/L	c	Q/2kL	x/L=0.0	x/L=0.2	x/L=0.4	x/L=0.6	x/L=0.8	x/L=1.0
0.01	1.8	0.00	0.000	0.012	0.00	0.0086	0.011	0.011	0.0085	0.00
0.01	1.8	0.05	0.083	0.012	0.00	0.0084	0.011	0.011	0.0084	0.00
0.01	1.8	0.20	0.319	0.011	0.00	0.0060	0.010	0.010	0.0082	0.00
0.01	1.8	0.40	0.592	0.0085	0.00	0.0023	0.0061	0.0084	0.0070	0.00
0.01	1.8	0.60	0.813	0.0057	0.00	0.0009	0.0020	0.0045	0.0053	0.00
0.01	1.8	0.80	0.950	0.0024	0.00	0.0002	0.0005	0.0009	0.0022	0.00
0.02	3.6	0.00	0.000	0.023	0.00	0.017	0.023	0.023	0.017	0.00
0.02	3.6	0.05	0.088	0.023	0.00	0.017	0.022	0.022	0.017	0.00
0.02	3.6	0.20	0.325	0.022	0.00	0.012	0.021	0.021	0.016	0.00
0.02	3.6	0.40	0.606	0.018	0.00	0.0044	0.012	0.018	0.015	0.00
0.02	3.6	0.60	0.813	0.012	0.00	0.0018	0.0041	0.010	0.012	0.00
0.02	3.6	0.80	0.950	0.0051	0.00	0.0005	0.0010	0.0018	0.0045	0.00
0.05	9.0	0.00	0.000	0.058	0.00	0.045	0.057	0.057	0.042	0.00
0.05	9.0	0.05	0.102	0.058	0.00	0.044	0.056	0.055	0.042	0.00
0.05	9.0	0.20	0.350	0.054	0.00	0.032	0.051	0.052	0.038	0.00
0.05	9.0	0.40	0.625	0.045	0.00	0.010	0.028	0.044	0.035	0.00
0.05	9.0	0.60	0.831	0.031	0.00	0.0040	0.0091	0.022	0.029	0.00
0.05	9.0	0.80	0.956	0.015	0.00	0.0010	0.0022	0.0041	0.014	0.00

Table 2 gives the values of $\psi_{max}/kL = Q/2kL$ as a function of α and a/L for the finite width between two hillsides problem. The values of $Q/2kL$ tend to increase for greater slopes just as they did for the infinitely width case. This table also gives the image point "c" values as needed for [40].

The geometry considered was for hillsides. On a smaller scale, the discussion is relevant to soil bedding and surface drainage for man-made surfaces. Curved water tables or fluctuating curved water tables beneath a sloping surface are perhaps more realistic boundaries and deserve further attention.

LITERATURE CITED

1. Abramowitz, M., and I. A. Stegun. 1964. Handbook of mathematical functions. Nat. Bur. Stand. Appl. Math. Ser., Vol. 55, US Gov. Printing Office, Washington, D.C.
2. Churchill, R. V. 1960. Complex variables and applications. 2nd ed. McGraw Hill Book Co., Inc., New York.
3. Davison, B., and L. Rosenhead. 1940. Some cases of the steady two-dimensional percolation of water through ground. Royal Soc. London Proc. 175 (Ser. A) 346-365.
4. Kirkham, D. 1947. Studies of hillside seepage in the Iowan drift area. Soil Sci. Soc. Amer. Proc. 12:73–80.
5. Klute, A., E. J. Scott, and F. D. Whisler. 1965. Steady-state water flow in a saturated inclined soil slab. Water Resour. Res. 1:287–294.
6. McCracken, D. D., and W. S. Dorn. 1964. Numerical methods and Fortran programming. John Wiley & Sons, Inc., New York.
7. Polubarinova-Kochina, P. Y. 1962. Theory of ground water movement. Princeton University Press, Princeton, N.J.
8. Powers, W. L., D. Kirkham, and G. Snowden. 1967. Orthonormal function tables and the seepage of steady rain through soil bedding. J. Geophysical Res. 72:6225–6237.
9. Selim, S., and D. Kirkham. 1972. Seepage through soil bedding or a hillside due to a steady rainfall. Parts 1 and 2. Soil Sci. Soc. Amer. Proc. 36:402–412.
10. Warrick, A. W. 1970. A mathematical solution to a hillside seepage problem. Soil Sci. Soc. Amer. Proc. 34:849–853.
11. Whisler, F. D. 1969. Analyzing steady-state flow in an inclined soil slab with an electric analog. Soil Sci. Soc. Amer. Proc. 33:19–25.